This paper was published in Proc. of SPIE, Volume 4725 – Algorithms and Technologies for Multispectral, Hyperspectral, and Ultraspectral Imagery VIII, Sylvia S. Shen, Paul E. Lewis, Editors, pp. 397-405, and is made available as an electronic reprint with permission of SPIE.

Cloud Remote Sensing with Sideways-Looks: Theory and First Results Using Multispectral Thermal Imager Data

Anthony B. Davis†
Los Alamos National Laboratory, Space & Remote Sensing Sciences Group (NIS-2)

ABSTRACT

In operational remote sensing, the implicit model for cloud geometry is a homogeneous plane-parallel slab of infinite horizontal extent. Each pixel is indeed processed as if it exchanged no radiant energy whatsoever with its neighbors. The shortcomings of this conceptual model have been well documented in the specialized literature but rarely mitigated. The worst-case scenario is probably high-resolution imagery where dense isolated clouds are visible, often both bright (reflective) and dark (transmissive) sides being apparent from the same satellite viewing angle: the low transmitted radiance could conceivably be interpreted in plane-parallel theory as no cloud at all. An alternative to the plane-parallel cloud model is introduced here that has the same appeal of being analytically tractable, at least in the diffusion limit: the spherical cloud. This new geometrical paradigm is applied to radiances from cumulus clouds captured by DOE's Multispectral Thermal Imager (MTI). Estimates of isolated cloud opacities are a necessary first step in correcting radiances from surface targets that are visible in the midst of a broken-cloud field. This type of advanced atmospheric correction is badly needed in remote sensing applications such as nonproliferation detection were waiting for a cloud-free look in the indefinite future is not a viable option.

Keywords: cloud remote sensing, three-dimensional radiative transfer, photon diffusion, surface remote sensing, cloud adjacency effects, advanced atmospheric correction schemes, Multispectral Thermal Imager, Earth radiation budget.

1. INTRODUCTION, CONTEXT AND OUTLINE

The only model for cloud geometry used in remote sensing operations is a horizontally-infinite/homogeneous plane-parallel slab. This is also true in climate studies where the emphasis is on radiative fluxes rather than radiances. This seems reasonable for satellite pixel-scales or model grid-scales that are large with respect to the thickness of the cloud layer, if such a well-defined layer indeed exists. However, more and more satellites can resolve much smaller scales; already we have LANDSAT, ASTER, MTI, SPOT, and a growing number of commercial assets. At their best resolutions (≈250 m), even MODIS and MISR resolve cloud radiances that are physically interdependent from pixel to pixel. Global climate models (GCMs) do not resolve scales less than a couple of hundred km, much more than the scale-height of the whole atmosphere (≈8 km), let alone a single cloud layer. With the proper cloud opacity variability folded in and the proper treatment of cloud overlap, plane-parallel theory might be brought to bear on GCM radiation budget estimation largely because only fluxes are of interest, not radiances. However, cloud-resolving models (CRMs) and Large-Eddy Simulations (LESs) are becoming very popular in climate research for process studies. These dynamical models resolve the scales where strong deviations from plane-parallel radiation transport are observed in satellite images, yet they use the same independent-column computations as GCMs.

The main reason for the popularity of such an extreme idealization of cloud shape and structure is that, in all the applications mentioned above, computer time is a concern either because of in high data flow in remote sensing operations or because of fierce competition for CPU time from other modules in GCMs, CRM, and LESs. Hence a requirement for analytical solutions, preferably in closed form, and plane-parallel slab geometry is the only one where these are readily available: "one-dimensional" radiative transfer theory. Needless to say, this modeling assumption introduces significant biases that have been studied extensively in the specialized literature using computationally intensive 3D radiative transfer models; see ref. 1 for a recent review. Another issue is that is not clear how to improve the situation. In particular, the 3D radiative transfer community has not been forthcoming with solutions, although there are a few notable exceptions.[2-4]

† adavis@lanl.gov; phone +1-505-665-6577; fax +1-505-667-9208; http://nis-www.lanl.gov/~adavis; LANL/NIS-2, P.O. Box 1663 (Mail Stop C-323), Los Alamos, New Mexico 87545, USA.

Algorithms and Technologies for Multispectral, Hyperspectral, and Ultraspectral Imagery VIII, Sylvia S. Shen, Paul E. Lewis, Editors, Proceedings of SPIE Vol. 4725 (2002)

A serious conceptual limitation of the slab-cloud model is that it partitions space into two disjoint half-spaces, one contains the Sun and open space, the other contains the Earth. With VIS/NIR wavelengths in mind, one can therefore view either reflected or transmitted light, never both, from any given point. This of course contradicts everyday observation of real horizontally-finite clouds from ground as well as from space with high enough spatial resolution and under large enough viewing angles. Thanks to its focal-plane design and its agility in orientation, MTI satisfies both of these conditions. I present here a new methodology for inferring the basic optical properties of dense compact clouds from radiometry that samples at once their bright and dark sides. It is based on an overlooked solvable case in 3D radiative transfer using the photon diffusion approximation: spherical clouds. This is a first step towards correction schemes for broken-cloud adjacency effects (shadowing and over-illumination). Such advanced correction schemes are needed to fully exploit modern satellite imagery in quantitative analyses, especially in national security applications were throwing away cloud-contaminated data (meaning maybe just 10-or-so % in radiometric accuracy) is not an option.

Isolated clouds have been investigated quite extensively in the 3D radiative transfer literature, although not much recently since attention as been shifted towards cloud layers with internal variability ranging from weak horizontal fluctuations to outright brokeness. For a comprehensive overview of current activity in computational 3D radiative transfer for atmospheric applications, the interested reader can look at the web-site of the NASA- and DOE-sponsored initiative in Intercomparison of 3D Radiation Codes (I3RC).[5] Isolated cloud models were used in the early atmospheric literature mostly for climate studies (where fluxes matter most); those studies I am aware of are listed in Table 1.

Cloud Geometry	**Diffusion Equation**	**Linear Boltzmann** (not by Monte Carlo)
plane-parallel slabs:	Schuster (1905)[6]	Chandrasekhar (1950)[7]
rectangular parallelepipeds:	Davies and Weinman (1977)[8], Davies (1978)[9]	Preisendorfer and Stephens (1984)[10], Stephens and Preisendorfer (1984)[11]
(upright) truncated cylinders:	Barkstrom and Arduini (1977)[12]	
spheres:	Giovanelli and Jefferies (1956)[13]	

Table 1. Cloud geometries used in the atmospheric radiation literature for the basic effects of finite horizontal extent —and the plane-parallel benchmark— using diffusion theory. References provided here are just for the solar problem of steady-state irradiation at certain boundaries by a collimated beam, a problem of considerable interest in climate studies. Only one or two early references are given in each case. Diffusion solutions are typically validated by comparison with straightforward Monte Carlo simulations by the same authors. These simulations amount to solving the linear Boltzmann equation but only for designated responses; in some cases, full (non-Monte-Carlo) solutions were obtained and they are indicated in the 3rd column. Time-dependent internal-source problems apply to lightning studies; see Koshak et al. (1994).[14] In this context, plane-parallel clouds were never an option because lightning is produced in towering convective clouds, not extensive stratus layers.

In the next section, we derive a simple relation for the ratio of reflected to transmitted flux integrated over their respective hemispheres on the surface of a spherical cloud in terms a harmonic expansion. In section 3, we obtain the required spherical harmonic coefficients explicitly in the photon diffusion limit (i.e., optically thick spheres). In section 4, we apply the diffusion result to estimate the optical density of isolated clouds in typical MTI imagery. We draw our conclusions in section 5 and look out to key applications.

2. SPHERICAL MEDIA UNDER UNIFORM ILLUMINATION: REFLECTION/TRANSMISSION

Following the proverbial path,[15] we consider a spherical cloud under uniform collimated illumination coming from the negative z direction and we take this to be the orientation of the polar axis. A priori the cloud can have internal structure as long as it is symmetric under rotation around the polar axis. In this case, radiation fields on the cloud's surface (at radius $r = constant$) are only functions of the polar position angle θ, and not of the azimuthal position angle φ. We are only interested here in the in-coming and out-going surface fluxes which we denote

$$F^{(\pm)}(\theta) = \sum_{n=0}^{\infty} (n+\tfrac{1}{2}) f_n^{(\pm)} P_n(\cos\theta) = \begin{cases} +: & \text{out - going flux} \\ -: & \text{in - coming flux} \end{cases}, \tag{1a}$$

using both angular and spherical-harmonic representations. The $f_n^{(\pm)}$ are coefficients in the spherical-harmonic expansion of the two surface-flux fields and $P_n(x)$, $-1 \le x \le +1$, are the Legendre polynomials; these coefficients are given by

$$f_n^{(\pm)} = \int_0^{\pi} F^{(\pm)}(\theta) P_n(\cos\theta) \sin\theta \mathrm{d}\theta \,. \tag{1b}$$

In the following, we will only need to know about the explicit expressions for

$$\begin{cases} P_0(x) = 1 \\ P_1(x) = x \end{cases} \tag{2}$$

to derive the final results. We know the characteristics of the in-coming flux field already:

$$F^{(-)}(\theta) = \begin{cases} 0, & 0 \le \theta \le \pi/2 \\ -F_0 \cos\theta, & \pi/2 \le \theta \le \pi \end{cases}, \tag{3a}$$

where F_0 is the solar constant. The first two spherical-harmonic coefficients for this field are therefore

$$\begin{cases} f_0^{(-)} = F_0/2 \\ f_1^{(-)} = -F_0/3 \end{cases}; \tag{3b}$$

at higher-orders, all the odd coefficients vanish identically. We anticipate the unknown out-going flux fields to have the same symmetry properties because they are linear *responses* to the boundary *source* term described in Eqs. (3a,b).

Turning to these out-going flux fields, we can compute hemispheric integrals recalling that the element of area on a sphere of radius r is $S(\mathrm{d}\theta) = \mathrm{d}S(\theta) = 2\pi r^2 \sin\theta \mathrm{d}\theta$. From the out-going flux field on the non-illuminated side of the cloud (cf. Eq. (3a)), we define the normalized mean transmitted flux, or "transmittance,"

$$T = \frac{1}{\pi r_c^2 F_0} \int_{\theta<\pi/2} F^{(+)}(\theta) \mathrm{d}S(\theta) = \frac{2}{F_0} \int_0^{\pi/2} F^{(+)}(\theta) \sin\theta \mathrm{d}\theta \tag{4}$$

where r_c is the (constant) radius of the cloudy medium. We can similarly obtain "reflectance" R just by changing the angular integration limits to $[\pi/2,\pi]$, again according to Eq. (3a).

The computation of R and T can be simplified and combined by introducing the Heaviside step-function for $\pm\cos\theta$,

$$\eta(\pm\cos\theta) = \sum_{n=0}^{\infty} (n+\tfrac{1}{2}) h_n^{\pm} P_n(\cos\theta) = \begin{cases} 1, & \pm\cos\theta \ge 0 \\ 0, & \text{otherwise} \end{cases}, \tag{5a}$$

along with its spherical-harmonic coefficients $h_n^{\pm}$. At orders 0 and 1, these are given by

$$\begin{cases} h_0^{\pm} = 1 \\ h_1^{\pm} = \pm 1/2 \end{cases}; \tag{5b}$$

for $n > 1$, all the odd-order coefficients vanish. Using the orthogonality relation for the Legendre polynomials,[16]

$$\int_{-1}^{+1} P_n(x) P_{n'}(x) \mathrm{d}x = \delta_{nn'} / (n+\tfrac{1}{2}) \tag{6}$$

where $\delta_{nn'}$ is the Kronecker symbol, we obtain

$$\begin{Bmatrix} T \\ R \end{Bmatrix} = \frac{1}{\pi r_c^2 F_0} \int_0^{\pi} F^{(+)}(\theta) \eta(\pm\cos\theta) \mathrm{d}S(\theta) = \frac{1}{F_0} \sum_{n=0}^{\infty} (2n+1) f_n^{(+)} h_n^{\pm} \tag{7}$$

for the (function-space) scalar product of $F^{(\pm)}(\theta)$ and $\eta(\pm\cos\theta)$. In fact, only the first two terms survive in (7) when we account for the symmetry properties of $F^{(\pm)}(\theta)$ and $\eta(\pm\cos\theta)$ discussed above. Using (5b), this leads to

$$\frac{R}{T} = \frac{1 - \frac{3}{2} f_1^{(+)} / f_0^{(+)}}{1 + \frac{3}{2} f_1^{(+)} / f_0^{(+)}} . \tag{8}$$

for the reflectance-to-transmittance ratio, a simple result we will now refine by obtaining $f_1^{(+)}/f_0^{(+)}$ from first principles.

3. CONSERVATIVE PHOTON DIFFUSION PREDICTION FOR *R/T*

In the bulk of optically dense media, we can accurately represent the radiance field $I(\boldsymbol{x},\Omega)$ at position $\boldsymbol{x}$ and in propagation direction Ω as a 2-term expansion in spherical harmonics with respect to Ω. It is important to not confuse this familiar *angular* expansion with the *positional* counterpart used above. So we have[17]

$$I(\boldsymbol{x},\Omega) \approx \tfrac{1}{4\pi}[J(\boldsymbol{x}) + 3\Omega \bullet \boldsymbol{F}(\boldsymbol{x})] \tag{9}$$

where the two new fields are

$$\begin{cases} \text{scalar flux:} & J(\boldsymbol{x}) = \oint I(\boldsymbol{x},\Omega)\mathrm{d}\Omega \\ \text{vector flux:} & \boldsymbol{F}(\boldsymbol{x}) = \oint \Omega I(\boldsymbol{x},\Omega)\mathrm{d}\Omega \end{cases} . \tag{10}$$

Vector flux $\boldsymbol{F}(\boldsymbol{x})$ appears in the *local* law of conservation of radiant energy which reads as

$$\nabla \bullet \boldsymbol{F} = 0 \tag{11}$$

in the absence of absorption and of volume-sources. In the terminology and notations introduced in Sect. 2, Eq. (11) leads to the *global* law of energy conservation expressed in normalized quantities as $T+R = 1$.[a]

The simplest way of introducing the photon diffusion approximation for radiation transport is to postulate Fick's law for photons:[18]

$$\boldsymbol{F} = -\frac{\ell_t}{3}\nabla J \tag{12}$$

where

$$\ell_t = \frac{1}{(1-g)\sigma} \tag{13}$$

is the "transport" mean-free-path (MFP). It is expressed here in terms of the extinction coefficient σ (or the usual MFP $1/\sigma$) and g, the scattering phase function "asymmetry factor" (mean cosine of the scattering angle), for conservative scattering to be congruent with Eq. (11).

If ℓ_t is uniform in the medium, we have

$$\nabla^2 J = 0 . \tag{14}$$

In other words, $J(\boldsymbol{x})$ obeys Laplace's equation. In spherical coordinates under azimuthal symmetry, such a harmonic function can be expressed as

$$J(r,\theta) = \sum_{n=0}^{\infty} j_n r^n P_n(\cos\theta) \tag{15}$$

---

[a] To show this note that $F^{\pm}(\boldsymbol{x})$, $\|\boldsymbol{x}\| = r_c$, are the inward and outward *hemispherical* components of the *net* flux across the surface of the cloud which is $\boldsymbol{n}(\boldsymbol{x})\bullet\boldsymbol{F}(\boldsymbol{x})$, $\boldsymbol{n}(\boldsymbol{x})$ being the outward normal vector.

using the standard separation of variables. We are interested here in the hemispherical fluxes at the boundary of the spherical turbid medium. In-going fluxes ("–" sign in superscript) are given by the mixed boundary conditions (BCs) used in photon diffusion theory.[17] These BCs are expressed as follows using the lower-level signs:

$$F^{(\pm)}(\theta) = \tfrac{1}{2}\left(1 \mp \chi \ell_{\mathrm{t}} \tfrac{\partial}{\partial r}\right) J(r,\theta)\Big|_{r=r_{\mathrm{c}}} . \tag{16}$$

The length-scale $\chi\ell_{\mathrm{t}}$ is called the "extrapolation length" in diffusion theory. The (essentially free) parameter χ is an $O(1)$ numerical constant that is traditionally used to match diffusion results with accurate solutions of the radiative transfer equation for the same geometry and illumination. Computing hemispherical fluxes using Eq. (9) leads to $\chi = 2/3$; the theoretical value based on the "Milne" benchmark problem is shown[17] to be $\chi = 0.7014\cdots$. At any rate, the upper-level signs in (16) give the out-going fluxes we seek.

Substitution of (15) into (16) yields

$$F^{(\pm)}(\theta) = \frac{1}{2}\sum_{n=0}^{\infty}\left(1 \mp n\chi\frac{\ell_{\mathrm{t}}}{r_{\mathrm{c}}}\right) j_n r_{\mathrm{c}}^n P_n(\cos\theta) . \tag{17}$$

This we identify, term-by-term (because of Legendre orthogonality), to Eq. (1a). This identification proves that there is indeed a one-to-one connection between the $f_n^{(+)}$, $f_n^{(-)}$ and j_n coefficients (as anticipated above) for all $n \geq 0$. We can easily write the results out explicitly for $n = 0,1$:

$$\begin{cases} f_0^{(\pm)} = j_0 \\ f_1^{(\pm)} = (1 \mp X) j_1 r_{\mathrm{c}} / 3 \end{cases}, \text{ where } X = \chi\frac{\ell_{\mathrm{t}}}{r_{\mathrm{c}}} . \tag{18}$$

Using Eq. (3b), we find

$$\left(\frac{3}{2}\right)\frac{f_1^{(+)}}{f_0^{(+)}} = -\frac{1-X}{1+X} \tag{19}$$

for the expression that appears twice in (8). Thus,

$$\frac{R}{T} = \frac{1}{X} = \frac{r_{\mathrm{c}}}{\chi\ell_{\mathrm{t}}} = (1-g)\frac{\tau}{2\chi} \tag{20}$$

where

$$\tau = \textit{optical}\ \text{diameter} = 2\sigma r_{\mathrm{c}} . \tag{21}$$

Recalling that $T+R = 1$, we can solve (20) for each response individually:

$$T = \frac{1}{1+(1-g)\tau/2\chi}, \; R = 1 - T . \tag{22}$$

Quite curiously, Eq. (22) is precisely the result of a diffusion-based calculation for a homogeneous plane-parallel slab if τ is its optical thickness; see Appendix for a derivation of the counterpart of (20) in slab geometry. Note that the segment $\{z \in \Re;\ |z| \leq r_{\mathrm{c}} = \tau/2\sigma\}$ is essentially a "sphere" in 1D. We therefore anticipate that the result in (22) also applies to a circle (i.e., a "sphere" in 2D) or, equivalently, an infinitely long cylinder illuminated on one side.

A slightly less rigorous derivation of (22) is given in ref. 19 where it is also generalized to a spherical medium containing a concentric cavity; this case is used to shed light on the basic effects of internal variability. Returning to Table 1, it is somewhat surprising that Giovanelli and Jefferies,[13] who investigated radiative diffusion in several geometries (including spheres and infinite cylinders), did not obtain the simple result in (22). This appears to be because they insisted on solving the problem fully but for quite general illumination conditions.

4. APPLICATION TO MTI RADIANCES

The angular distribution of radiance escaping opaque non-absorbing media such as clouds, snow, white paint, and so on, is approximately isotropic, as for a Lambertian ground surface. This means that a typical radiance emanating from the transmission and reflection sides of a cloud are given approximately by

$$I_R \approx F_0 R / \pi,\ I_T \approx F_0 T / \pi\ . \tag{23}$$

There is no need for the usual cosine of the solar zenith angle here because it was used already in (3a). At this point, we are not fundamentally interested in where the ground is with respect to the cloud.

Equation (20) can now be turned around and used as a means to infer the optical thickness of an isolated cloud where the ratio *R/T* can be estimated from a single look:

$$\tau_{\text{eff}} = \left(\frac{2\chi}{1-g}\right)\left.\frac{R}{T}\right|_{\text{equivalent sphere}} \approx \left(\frac{2\chi}{1-g}\right)\frac{I_R}{I_T} \approx 9.47\,\frac{I_R}{I_T}\ . \tag{24}$$

We have made use here of the fact that $\chi \approx 0.71$ is a well-accepted value and that g is known to be quite uniform in boundary-layer (liquid-water) clouds at ≈ 0.85. Figure 1 summarizes the basic steps in cloud remote-sensing using both sides of a clouds with respect to its direction of illumination. Having identified a cloud of interest in an image, it is important to not take extreme values of radiance on the darker and brighter sides, but rather to take "typical" values since the theory calls for a ratio of overall means. Also, we are careful in Eq. (24) to call the retrieved optical depth the "effective" optical depth for the "equivalent sphere" that would have the same *R/T* ratio as is observed. Note that there is no difference in this detailed qualification of the remote sensing result with the one that should accompany results using the plane-parallel model in a one-wavelength retrieval. Indeed, one obtains (only) the "effective" optical depth for the "equivalent plane-parallel slab" that would have the same *R* as is observed from space, or *T* from ground.[20,21]

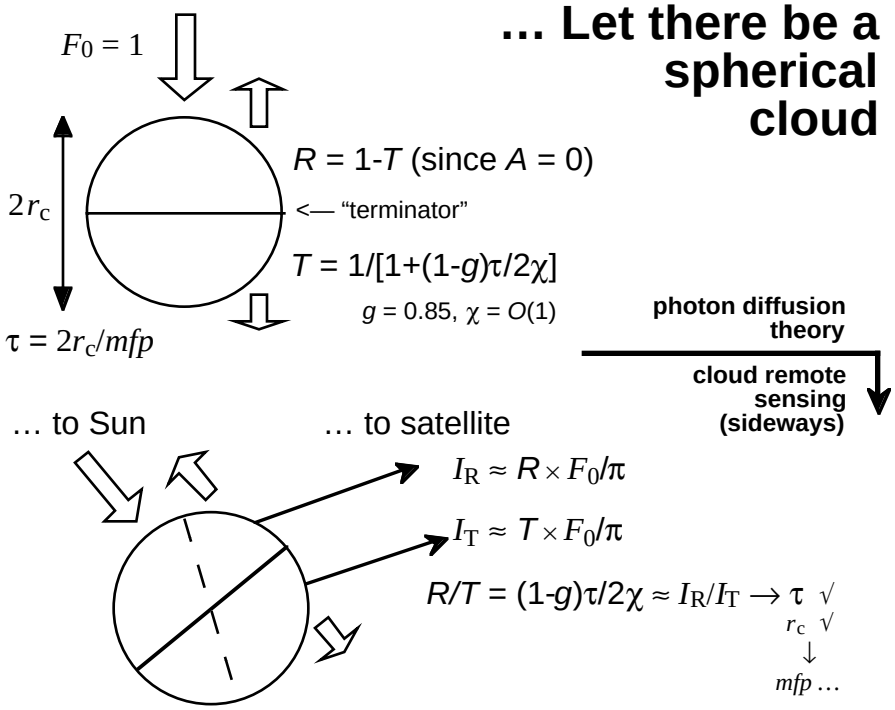

Figure 1. Schematic of cloud remote sensing from a sideways look where both reflected and transmitted light can be seen using a single non-absorbed wavelength. Physical cloud size, r_c, is easily obtained for isolated clouds, hence the MFP and extinction.

Figure 2 is an MTI scene of Los Alamos (35.875 N, 106.324 W), NM, USA, collected on 2000-09-22 at 19:05 UTC. A basic geo-rectification was done by rotating the off-nadir aft-direction push-broom capture by 180 degrees (for the clouds' sunny sides to be upwards), then compressing the vertical axis by 1/2 (roughly the cosine of the viewing zenith angle). Cloud droplets are essentially non-absorbing in all three high (5-m) resolution VIS bands used here (channels A, B, C) as well as in their NIR counterpart (channel D). This is all we need to know to apply the cloud remote-sensing technique proposed in this paper; see ref. 22 for detailed band and other specifications of the instrument. Table 2 summarizes the sampling performed on the data as indicated in Fig. 2. It shows that the simple formula in (24) gives reasonable results for these cumulus to within an uncertainty estimated at 20-30% which, incidentally, is no worse than in standard cloud remote sensing. Independent validation of the algorithm, and possible refinements, will be the object of future work.

Figure 2. Gray-scale version rendering of a "true-color" channel combination of an MTI scene of Los Alamos (NM) in the presence of broken clouds. This is a 57.4 degree off-nadir look in the aft direction (i.e., from a position to the North). For visual comfort, it is corrected for pixel aspect ratio and orientation to mimic an airborne vista. The Sun, at 54 degrees from zenith, is about 175 degrees away from the viewing direction in azimuth. The positions of cloudy regions that were used to compile the statistics in Table 2 are highlighted. Cloud-to-cloud radiative interactions are neglected.

Cloud →	"Big"		"Medium"		"Small"	
"D" data ↓	*R*-region	*T*-region	*R*-region	*T*-region	*R*-region	*T*-region
mean:	255.89	58.091	257.37	56.816	195.79	70.770
st-dev/mean (%):	2.1	11	6.0	5.5	7.6	5.4
minimum:	244.40	45.861	228.34	51.128	167.00	65.461
maximum:	272.33	70.634	282.50	66.459	227.21	82.429
# of pixels (-):	272	624	132	340	81	120
I_R/I_T range (-):	3.5–5.9		3.4–5.5		2.0–3.5	
τ_{eff} range (-):	33–56		33–52		19–33	

Table 2. Sampling results for the 3 pairs of regions-of-interest in the MTI image in Fig. 2 for the broken/isolated cloud case-study. Radiance units are $W/m^2/st/\mu m$. We show only data from channel D which is in the near IR as it has the least contamination by aerosol and molecular scattering. Results using the other (visible) channels are very similar as can be expected from the simple fact that clouds are uniformly reflective —essentially white— across the solar spectrum.

5. CONCLUSIONS AND OUTLOOK

I have derived a simple formula for the area-averaged and normalized transmitted flux T for a spherical non-absorbing turbid medium under collimated illumination in terms of its optical diameter, τ = diameter/mean-free-path, and the asymmetry factor of the scattering phase function g, which is ≈0.85 for boundary-layer clouds. The formula for ratio of cloud albedo $R = 1–T$ to T is even simpler: $R/T = (1–g)\tau/2\chi$ where χ is an $O(1)$ numerical constant ≈2/3. The photon diffusion transport model used to derive these results is valid when $(1–g)\tau \approx R/T \gtrsim 1$. Under an assumption of Lambertian reflection and transmission, this result can be used derive τ (for an "equivalent" sphere) from radiances emanating from the dark/shady and bright/sunny sides of clouds in satellite imagery at high-enough resolution.

The method gives satisfactory, although preliminary, results with MTI data. We will be devising methods of validating this new retrieval in the near future. In the more distant future, estimation of isolated cloud opacity will become a first step in the correction of remote-sensing data for cloud-adjacency effects. This is the equivalent of a quantum leap in atmospheric correction technology and one that is needed more in nonproliferation monitoring than in remote sensing for the purposes of environmental monitoring (as in a global change program). This is because in the latter applications it is generally acceptable to wait a couple of weeks for a more cloud-free data acquisition; this may not be an option when a crisis situation is developing in a region under close surveillance. So cloud-capable atmospheric correction of the remote-sensing data down to its inherent noise-level is a worthy long-term goal as well as a challenge for 3D atmospheric radiative transfer.

APPENDIX: *R/T* FOR CONSERVATIVE PHOTON DIFFUSION IN SLAB GEOMETRY

Equation (14), $\nabla^2 J \equiv J''(z) = 0$ in this 1D case, says simply that $J(z)$ is a linear function of z:

$$J(z) = J_0 + J_1 z. \tag{A1}$$

But we will not need to determine the constants to compute the ratio R/T.

The BCs look like Eq. (16), using lower signs, but without the θ-dependence. However, in Cartesian coordinates, the signs on the right-hand side of (16) are flipped when going between the illuminated and the non-illuminated boundaries. Specifically, for an "illumination" BC (with incoming flux $F_0 = 1$) and reflection at $z = H$ (the *physical* thickness of the plane-parallel cloud) and just transmission at $z = 0$ (also called an "absorbing" BC), we have

$$\begin{cases} \frac{1}{2}\left[1 + \chi\ell_t \frac{\partial}{\partial z}\right] J\Big|_{z=H} = 1 \\ \frac{1}{2}\left[1 - \chi\ell_t \frac{\partial}{\partial z}\right] J\Big|_{z=0} = 0 \end{cases}, \tag{A2}$$

where ℓ_t and χ have the same meanings as in (13) and (16) respectively. The two responses of interest are now

$$\begin{cases} R = \frac{1}{2}\left[1 - \chi\ell_t \frac{\partial}{\partial z}\right] J\Big|_{z=H} \\ T = \frac{1}{2}\left[1 + \chi\ell_t \frac{\partial}{\partial z}\right] J\Big|_{z=0} \end{cases}. \tag{A3}$$

From (A1) and (A3), their ratio is

$$\frac{R}{T} = \frac{J_0 + (H - \chi\ell_t)J_1}{J_0 + \chi\ell_t J_1}. \tag{A4}$$

From (A2), lower BC, we have $J_0 = J_1\chi\ell_t$. Substituting this into (A4) yields

$$\frac{R}{T} = \frac{H}{2\chi\ell_t} = \frac{(1-g)\tau}{2\chi}, \tag{A5}$$

which is the equivalent of (20). Indeed, we can map H to the diameter $2r_c$ of the sphere since the *optical* thickness of slab is σH, where σ is again the uniform extinction (i.e., 1/MFP). Therefore Schuster's formula in (22), first derived[6] for the plane-parallel slab, applies to both geometries as long as the appropriate meaning of τ is kept in mind.

ACKNOWLEDGMENTS

The author acknowledges DOE/NN-20 for ongoing support as member of the MTI Science Team. He also thanks Drs. R. Cahalan, P. Chylek, R. Davies, F. Evans, P. Gabriel, D. Levermore, T. Light, K.–N. Liou, S. Lovejoy, A. Marshak, K. Pfeilsticker, I. Polonsky, G. Stephens, J. Weinman, and W. Wiscombe for many fruitful discussions on 3D radiative transfer through clouds in general and by diffusion in particular.

REFERENCES

1. A. B. Davis, and A. Marshak, "Multiple scattering in clouds, insights from three-dimensional diffusion/P_1 theory," *Nucl. Sci. Eng.* **137**, pp. 251-288, 2001.
2. A. Marshak, A. Davis, R. F. Cahalan, and W. J. Wiscombe, "Nonlocal independent pixel approximation: Direct and inverse problems," *IEEE Trans. Geosc. and Remote Sens*. **36**, pp. 192-205, 1998.
3. A. Marshak, Y. Knyazikhin, A. B. Davis, W. J. Wiscombe, and P. Pilewskie, "Cloud - vegetation interaction: Use of normalized difference cloud index for estimation of cloud optical thickness," *Geophys. Res. Lett.* **27**, pp. 1695-1698, 2000**.**
4. T. Faure, H. Isaka, and B. Guillemet, "Neural network retrieval of cloud parameters of inhomogeneous and fractional clouds: Feasibility study," *Remote Sens. Environ.* **77**, pp. 123-138, 2001.
5. http://climate.gsfc.nasa.gov/I3RC/intro.html
6. A. Schuster, "Radiation through a foggy atmosphere," *Astrophys. J*. **21**, pp. 1-22, 1905.
7. S. Chandrasekhar, *Radiative Transfer*, Oxford University Press, 1950, reprinted by Dover, New York (NY), 1960.
8. R. Davies, and J. A. Weinman, "Results from two models of the three dimensional transfer of solar radiation in finite clouds," in *Radiation in the Atmosphere*, ed. H.-J. Bolle, Science Press, Princeton (NJ), pp. 225–227, 1977.
9. R. Davies, "The effect of finite geometry on the three-dimensional transfer of solar irradiance in clouds," *J. Atmos. Sci.* **35**, pp. 1712-1725, 1978.
10. R. W. Preisendorfer, and G. L. Stephens, "Multimode radiative transfer in finite optical media, I: Fundamentals," *J. Atmos. Sci.* **41**, pp. 709-724, 1984.
11. G. L. Stephens, and R. W. Preisendorfer, "Multimode radiative transfer in finite optical media, II: Solutions," *J. Atmos. Sci.* **41**, pp. 725-735, 1984.
12. B. R. Barkstrom, and R. F. Arduini, "The effect of finite size of clouds upon the visual albedo of the Earth," in *Radiation in the Atmosphere*, ed. H.-J. Bolle, Science Press, Princeton (NJ), pp. 188-190, 1977.
13. R. G. Giovanelli, and J. T. Jefferies, "Radiative transfer with distributed sources," *Lond. Phys. Soc. Proc.* **69**, pp. 1077-1084, 1956.
14. W. J. Koshak, R. J. Solakiewicz, D. D. Phanord, and R. J. Blakeslee, "Diffusion model for lightning radiative transfer," *J. Geophys. Res.* **99**, pp. 14361-14371, 1994.
15. J. Harte, *Consider a Spherical Cow - A Course in Environmental Problem Solving*, William Kaufmann Inc., Los Altos (Ca), 1985.
16. M. Abramowitz, and I. A. Stegun (Eds.), *Handbook of Mathematical Functions with Formulas, Graphs, and Mathematical Tables*, U.S. Govt. Print. Off., Washington (DC), 1964, reprinted by Dover, New York (NY), 1975.
17. K. M. Case, and P. F. Zweifel, *Linear Transport Theory*, Addison-Wesley Publ. Co., Reading (Ma), 1967.
18. F. Rief, *Fundamentals of Statistical and Thermal Physics*, McGraw-Hill, New York (NY), 1965.
19. A. Davis, *Radiation Transport in Scale-Invariant Optical Media*, PhD Thesis, McGill University, Physics Department, Montreal (Qc), 1992.
20. E. Leontieva, and K. Stamnes, "Remote sensing of cloud optical properties from ground-based measurements of transmittance: A feasibility study," *J. Appl. Meteor*. **35**, pp. 2012-2022, 1996.
21. Q.-L. Min, and L. C. Harrison, "Cloud properties derived from surface MFRSR measurements and comparison with GOES results at the ARM SGP site," *Geophys. Res. Lett.* **23**, pp. 1641-1644, 1996.
22. J. J. Szymanski, W. H. Atkins, L. K. Balick, C. C. Borel, W. B. Clodius, R. Christensen, A. B. Davis, J. C. Echohawk, A. E. Galbraith, K. L. Hirsch, J. B. Krone, C. K. Little, P. M. McLachlan, A. Morrison, K. Pollock, P. Pope, C. Novak, K. Ramsey, E. Riddle, C. A. Rohde, D. C. Roussel-Dupre, B. W. Smith, K. Smith, K. Starkovich, J. Theiler, and P. G. Weber, "MTI science, data products, and ground-data processing overview," in *S.P.I.E. Proceedings*, *vol. 4381: Algorithms for Multispectral, Hyperspectral, and Ultraspectral Imagery VII,* eds. S. S. Shen and M. R. Descour, pp. 195-203, 2001.